J. Chem. Sci., Vol. 118, No. 6, November 2006, pp. 593–600.

Nanostructured metal particle-modified electrodes for electrocatalytic and sensor applications

RAMASAMY RAMARAJ

Centre for Photoelectrochemistry, School of Chemistry, Madurai Kamaraj University, Madurai 625 021
e-mail: ramarajr@yahoo.com

Abstract. Nanotechnology has become one of the most exciting frontier fields in analytical chemistry. The huge interest in nanomaterials, for example in chemical sensors and catalysis, is driven by their many desirable properties. Although metal is a poor catalyst in bulk form, nanometre-sized particles can exhibit excellent catalytic activity due to their relative high surface area-to-volume ratio and their interface-dominated properties, which significantly differ from those of the bulk material. The integration of metal nanoparticles into thin film of permselective membrane is particularly important for various applications, for example in biological sensing and in electrocatalysis. We have already established different techniques to design permselective membrane-coated chemically modified electrodes with incorporated redox molecules for electrocatalytic, electrochromic and sensor applications. Recently, we have prepared nanostructured platinum and copper (represented M_{nano}, M = Pt and Cu) modified GC/Nafion electrodes (GC/Nf/M_{nano}) and characterized by using AFM, XPS, XRD and electrochemical techniques. The nanostructured M_{nano} modified electrodes were utilized for efficient electrocatalytic selective oxidation of neurotransmitter molecules in the presence of interfering species such as ascorbic acid (AA) and uric acid (UA). It has been also shown that the modified electrodes could be used as sensors for the detection of submicromolar concentrations of biomolecules with practical applications to real samples such as blood plasma and dopamine hydrochloride injection solution. The GC/Cu_{nano} electrode has been used for catalytic reduction of oxygen.

Keywords. Metal nanoparticles; platinum; copper; Nafion$^{@}$; modified electrode; electrocatalysis; sensor.

1. Introduction

Nanoparticles-on-electrodes comprise a fundamentally interesting class of materials, in part because of an apparent dichotomy which exists between their sizes and many of their physical and chemical properties.[1-5] In the electrodeposition of metal particles, the most common method involves the reduction of appropriate metal salts in the presence of stabilizers such as polymers, surfactants or special ligands which prevent undesired formation of insoluble bulk metal particles. Nanoparticles could facilitate electron transfer reactions and this coupled with an ease of miniaturization of sensing devices to nanoscale dimensions make nanoparticles suitable for important applications in chemical/biochemical sensing because of their high surface-to-volume ratio and highly effective catalytic properties.[1–8] In particular, platinum (Pt) nanoparticles has been an intensive research subject for the design of nanostructured electrodes. The combination of the electronic conductivity and electroactivity of metal nanoparticles with high ionic conductivity and ion-exchange capacity of Nafion$^{@}$ (Nf) provides much scope for the design of nanoparticles on Nf film modified electrodes with novel properties and applications.[9-13] Electrocatalytic reactions are of central importance in electrochemistry and play a vital role in emerging technologies related to environmental and energy-related applications.[1–14] Pt-group nanoparticles in the size range of 2–10 nm, employed commercially in fuel cells and related applications, exhibit various interesting electronic and coordinative properties.[15]

Oxygen reduction has been widely studied in both acidic and basic electrolyte solutions because of its fundamental importance in electrochemistry and also in fuel cell applications.[16–20] On the other hand, its reduction in neutral solution is interesting in the development of biosensors for dissolved oxygen in biological processes. Metal microparticles deposited on electrode surfaces with and without polymer coatings and their resulting electrocatalytic properties have been reported.[21,22] Polymer films, such as poly(4-vinylpyridine) and polypyrrole, enhance the

stability and dispersity of the embedded Pt particles on GC electrodes. Use of deposited metal particles for both hydrogen evolution and oxygen reduction has been investigated.[21–23]

Dopamine (DA) is one of the most significant catecholamines and belongs to the family of excitatory chemical neurotransmitters.[24–27] The important challenges to measure DA under physiological conditions utilizing electrochemical methods are: the very low concentration levels of DA (in the submicromolar range) and the intensive interference arising from the electroactive ascorbate (AA) that is present at relatively high concentrations (0·2–0·5 mM). These problems exist due to the very close oxidation potentials of DA and its metabolites and AA at the bare electrodes. Several reports have demonstrated that the films such as Nafion,[28] clay,[29] melanin polymer[30] at physiological could attract and preconcentrate biomolecules such as cationic DA while effectively rejecting the anionic AA and other anionic interfering agents. This paper mainly presents some of our recent work[31–35] on the applications of nanostructured Pt and Cu electrodeposited on plain and Nf film coated electrodes for the simultaneous detection and determination of biomolecules in the presence of interference molecules and the reduction of oxygen. These metal nanoparticle-modified electrodes, coupled with the permselective Nf membrane, promote the adsorption and electron-transfer reactions of substrate molecules.

2. Electrochemical deposition of nanostructured platinum and copper on electrode

Electrodeposition of nanostructured Pt on the Nf or clay (bentonite clay) film coated glassy carbon (GC) and indium tin oxide (ITO) electrodes were carried out by electrochemical methods.[36] Nf films were coated on GC and ITO electrodes by transferring known volume of Nf or clay solution on the electrode surface and allowing the solvent to evaporate at room temperature. Subsequently, the GC/Nf and GC/clay electrodes were kept in distilled water for 30 min. Thicknesses of the Nafion and clay films were calculated by knowing the density of 1·58 g/cm^3 for Nafion[37] and 1·77 g/cm^3 for clay.[38] The electrodes (GC, GC/Nf, GC/clay, ITO and ITO/Nf) were dipped in a mixture of deaerated 1 M H_2PtCl_6 and 1 M $HClO_4$ solution for 5 min followed by continuous scanning of the electrodes between the potentials 1·0 and –0·1 *V*(SCE) to deposit Pt particles onto the electrodes. The electrodes were washed and dipped in distilled water and used for electrochemical experiments (referred as GC/Pt_{nano}, GC/Nf/Pt_{nano}, GC/clay/Pt_{nano}, ITO/Pt_{nano} and ITO/Nf/Pt_{nano}). These metal nanoparticle-modified electrodes were used for oxygen reduction and simultaneous detection and determination of biomolecules. Nanostructured copper particles were deposited electrochemically on GC and ITO electrodes (GC/Cu_{nano} and ITO/Cu_{nano}) using deaerated solutions of 0·01 M $CuSO_4$ and 0·1 M $NaClO_4$ under different applied potentials (E_{app} = 0·0 to −0·6 *V*(SCE)). Better electrocatalytic activity could be achieved when Cu_{nano} was electrodeposited at –0·4 V at a charge of 700°C.

3. Characterization of Pt_{nano} and Cu_{nano} modified electrodes

The continuous cyclic voltammograms recorded between 1·0 and −0·1 V at a scan rate of 10 mV/s for GC, GC/Nf and GC/clay electrodes dipped in 1 M H_2PtCl_6 and 1 M $HClO_4$ are shown in figure 1.[31,32] In

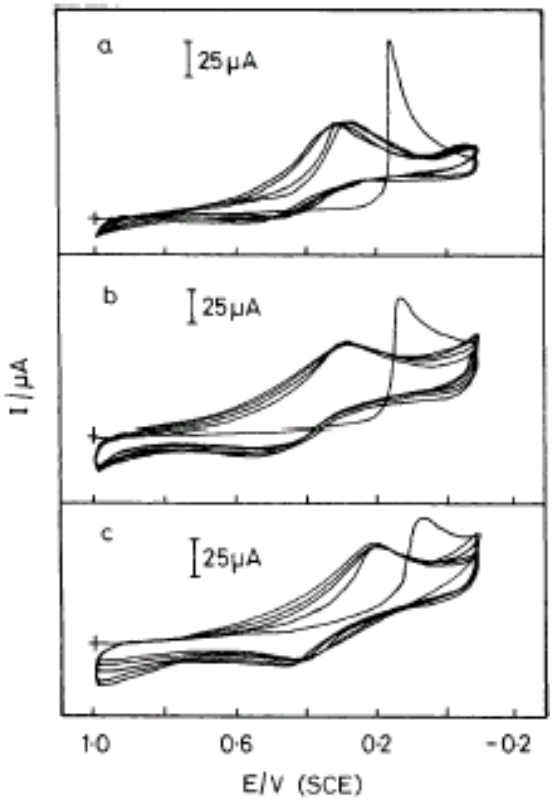

Figure 1. Continuous cyclic voltammograms of (**a**) GC, (**b**) GC/Nf and (**c**) GC/BT electrodes in deaerated 1 M H_2PtCl_6 and 1 M $HClO_4$. Scan rate = 10 mV/s.

the first scan the four-electron reduction of Pt(IV) to Pt(0)[39] occurred at 0·1 V (figure 1).[31,32] In subsequent cycles, the peak current at 0·1 V disappeared and a new irreversible reduction peak was observed at 0·3 V. This indicates that the deposition of Pt particles occurred in the first cycle and Pt underwent oxidation at > 0·5 V in the oxidative scan.[31,32]

The electrochemical properties of nanostructured Pt were studied at different pH in the range 1–7. The reduction peak potential of Pt was found to be dependent on the solution pH.[33,34] Figure 2 shows the PtO reduction peak potentials recorded for GC/Nf/Pt_{nano} electrode at varying pH. The irreversible reduction peak potential shifts to more negative potentials and the reduction peak potentials fit well to a straight line in the pH range 1·0 to 7·0 (figure 2), while the slope of the straight line is found to be 59 mV/pH. The shift in the peak potential with respect to pH has been attributed to proton-coupled reaction, (1). The intercept value of 0·4 V (figure 2) confirms the reduction behaviour of the Pt_{nano} deposited on the GC/Nf electrode.[33,34]

$$PtO + 2e^- + 2H^+ \rightarrow Pt + H_2O. \quad (1)$$

The AFM image recorded for the ITO/Nf/Pt_{nano} electrode is shown in figure 3. The Pt_{nano} are homogeneously distributed on the electrode surface forming a densely packed film and each particle is in contact with adjacent ones. The electrodeposition of Pt_{nano} leads to the formation of nanostructured Pt_{nano} with smaller grains in the range 25–50 nm and larger aggregates of about 500 nm.[33,34] The Pt_{nano} deposited on the electrode was also characterized by X-ray photoelectron spectroscopy (figure 4) and X-ray diffraction studies.[33,34]

Figure 4 shows the XPS obtained for the Pt_{nano} deposited on the Nf film coated electrode. The peak with binding energy of 71·2 eV is assigned to the presence of Pt.[40,41] The peak at 74·8 eV is more difficult to assign because bulk PtO_2 and $Pt(OH)_4$ show similar binding energies[40,41] (74·7 and 74·3 eV, respectively).

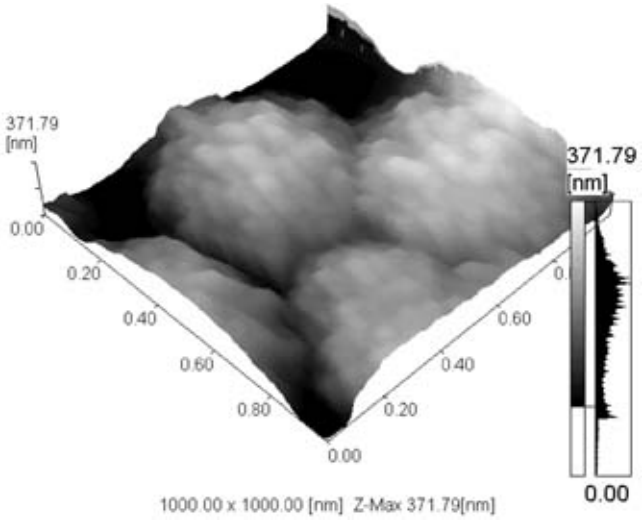

Figure 3. Tapping-mode 3D AFM image (1 μm × 1 μm) of ITO/Nf/Pt_{nano} electrode surface.

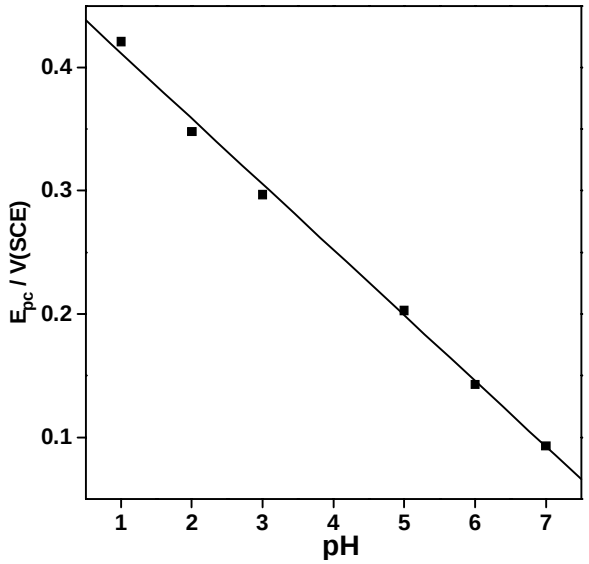

Figure 2. Plot of pH against the cathodic peak potential (E_{pc}) for GC/Nf/Pt_{nano} electrode.

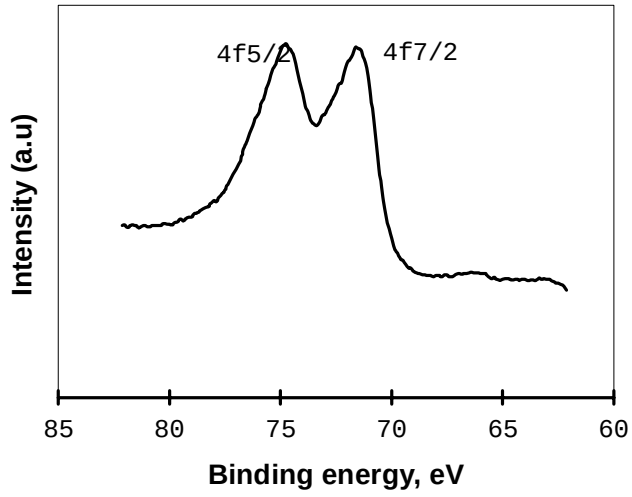

Figure 4. XPS of Pt($4f_{7/2\text{-}5/2}$) core-level spectra of electrodeposited Pt_{nano} on the ITO/Nf electrode (ITO/Nf/Pt_{nano}).

The AFM image of nanostructured Cu deposited Nf film-coated ITO electrode (ITO/Nf/Cu_{nano}) is shown in figure 5. The sizes of the aggregates measured from the cursor plot vary from 20 to 200 nm. This observation shows that the electrodeposition of Cu_{nano} leads to the formation of nanostructured Cu particles with smaller grains in the range 15–25 nm and larger aggregates in the range 130–200 nm. The Cu_{nano} formed on the electrode was also characterized by X-ray photoelectron spectroscopy and X-ray diffraction studies.[34,35] The emission of 2*p* photoelectrons from Cu is identified in two peaks of the XPS spectra, one is assigned to Cu(0) (935 eV) and the other one to Cu(I) (955 eV). The observed Cu(2*p*) binding energies indicate the presence of Cu(0) and Cu(I) ($Cu^{I}_{2}O$) species.[42]

4. Oxygen reduction at nanostructured Pt modified electrode

Cyclic voltammograms recorded for GC/Pt, GC/Nf/Pt_{nano} and GC/clay/Pt_{nano} electrodes dipped in oxygenated 0·1 M H_2SO_4 showed an irreversible reduction peak at 0·4 V with increased cathodic peak current when compared to plain GC electrode. When the potential range was increased from 0·6 to 1·3 V while running the cyclic voltammograms an increase in the cathodic peak current was observed at 0·4 V. This observation showed that the PtO formed at the Pt_{nano} deposited electrode was involved in the O_2 reduction process. The partial reduction product was found to be hydrogen peroxide (H_2O_2). This indicates that the O_2 undergoes two-electron reduction to the H_2O_2 at PtO-covered Pt_{nano} deposited electrode in addition to the four-electron reduction of O_2 to water (figure 6).[31,32]

The O_2 reduction reaction on Pt_{nano} proceeded through a pathway involving the adsorption of O–O and decomposition of O–O bond.[43] In our work[31,32] the PtO covered Pt_{nano} electrode favoured the partial desorption of the two-electron reduction product H_2O_2 into the solution. The adsorbed H_2O_2 was much more readily desorbed from the site on PtO than from the adsorption site involved in the four-electron reduction process at Pt_{nano} (figure 7).

The amounts of H_2O_2 were measured at an applied potential of 0·4 V using the Pt_{nano} modified electrodes at different time intervals and the results are shown in figure 8.[31,32] At an applied potential of 0·4 V (using the anodized GC/Pt_{nano}, GC/Nf/Pt_{nano} and GC/clay/Pt_{nano} electrodes at > 1·0 V), the amounts of H_2O_2 were observed as 0·0, 0·031, 0·053 and 0·045 μmoles in 30 min, respectively. The analysis of the charge accumulated at the O_2 reduction potential (0·4 V) showed that ~ 40% of the conversion of O_2 to H_2O_2 occurred at the PtO covered Pt_{nano} deposited electrodes. At 30 min, the PtO might undergo reduction to Pt_{nano} at 0·4 V in addition to the PtO

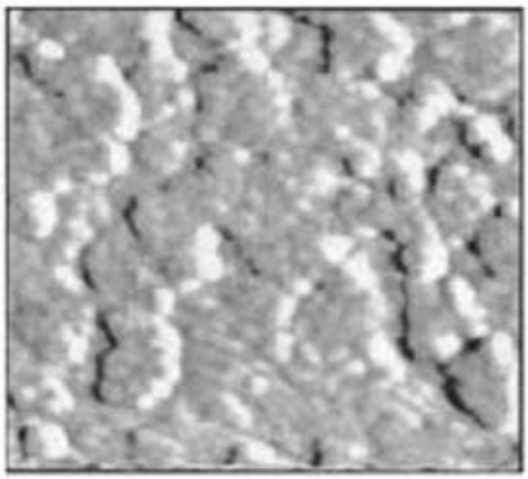

Figure 5. Tapping mode of 2D AFM image (1·0 μm × 1·0 μm) of ITO/Nf/Cu_{nano} electrode surface.

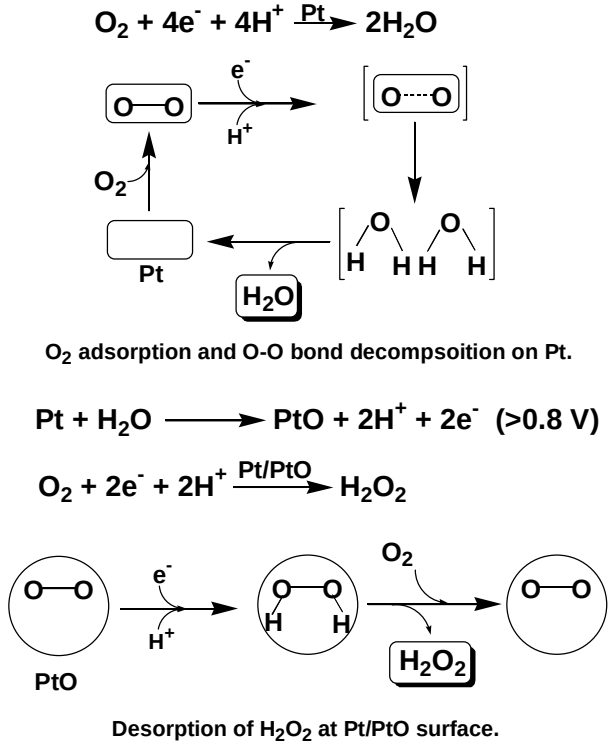

Figure 6. Schematic representation of O_2 reduction reactions at Pt_{nano} and Pt_{nano}/PtO modified electrode.

catalysed O_2 reduction and the amount of formation of H_2O_2 reached a maximum. When Pt_{nano} at the modified electrodes was again anodized, PtO catalysed reduction of O_2 to H_2O_2 was observed.[31,32]

5. Simultaneous detection of biomolecules at nanostructured Pt modified electrode

Figure 9 shows the anodic DPV responses of 100 μm DA at the plain GC, GC/Pt_{nano} and GC/Nf/Pt_{nano} electrodes in phosphate buffer (pH 7·2). The oxidation of DA appeared at 0·13 V at GC/Nf/Pt_{nano} electrode. A shift of about 60 mV to more negative potential for DA was observed at GC/Nf/Pt_{nano} when compared to plain GC electrode with an 11·6 fold enhancement of peak current (figures 9a and c). The electrochemical deposition of Pt_{nano} on Nf film-coated electrode (GC/Nf/Pt_{nano}) (figures 9b and c) increases the anodic peak current of DA when compared to the GC/Pt_{nano} electrode. The voltametric experiments were also carried out using the GC/Nf/Pt_{nano} electrode with different concentrations of DA and the peak current was found to be proportional to the concentration of dopamine in the range from 3×10^{-6} – 60×10^{-6} M DA with a detection limit of 10 nM.[33,34]

Ascorbic acid (AA) and uric acid (UA) are the important interference molecules in the measure-

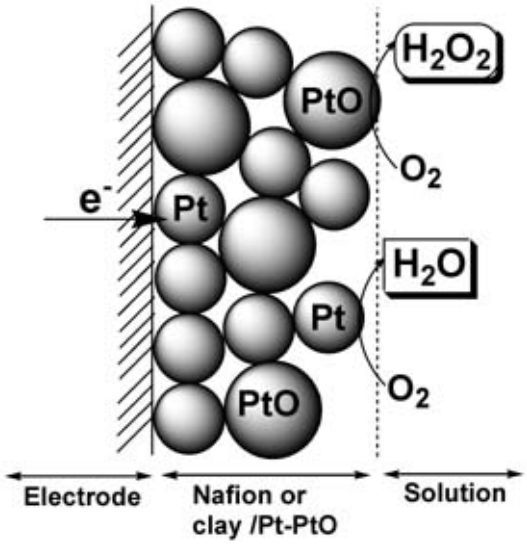

Figure 7. Schematic representation of O_2 reduction to H_2O and H_2O_2 at PtO covered Pt_{nano} deposited GC electrode. (Before O_2 reduction experiment, the Pt_{nano} modified electrode was oxidized at > 0·8 V.)

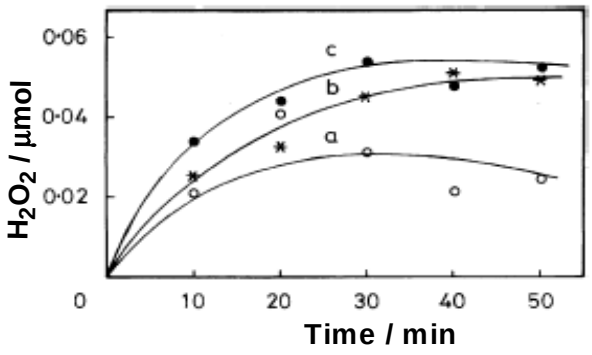

Figure 8. Amounts of H_2O_2 formed at the anodized GC/Pt_{nano} (a), GC/Nf/Pt_{nano} (b) and GC/clay/Pt_{nano} (c) electrodes at an applied potential of 0·4 V dipped in oxygenated 0·1 M H_2SO_4.

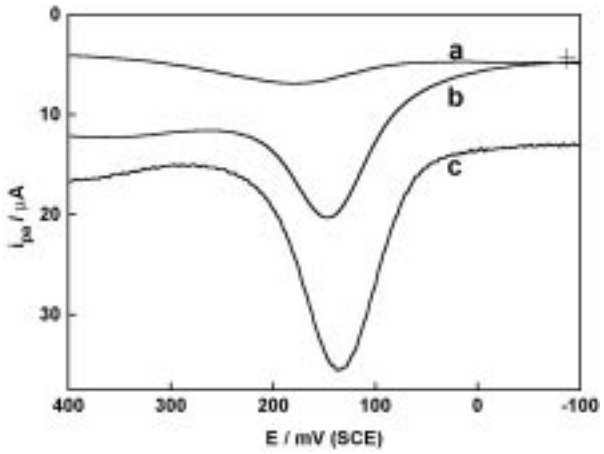

Figure 9. Anodic DPVs recorded for 100 μM DA at plain GC (a), GC/Pt_{nano} (b) and GC/Nf/Pt_{nano} (c) electrodes in 0·1 M phosphate buffer (pH 7·2).

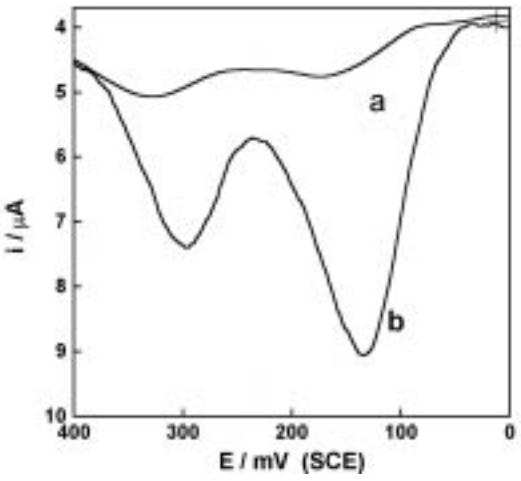

Figure 10. Anodic DPVs recorded at GC/Nf (a) and at GC/Nf/Pt_{nano} electrode (b) in 0·1 M PBS for a mixture of 50 μM DA and 500 μM 5-HT in presence of 1·0 mM AA and 0·1 mM UA.

ment of DA in biological systems and the oxidation potential of AA and UA are very close to that of DA. It has been demonstrated that Nf film is a sufficient barrier for several anionic interfering analytes and acts as a permselective membrane.[24] Figure 10a clearly shows that the GC/Nf electrode is very effective in rejecting anions such as AA and UA and better peak separation for the mixture of DA and serotonin (5-HT) was also observed in the presence of higher concentrations of interferences such as AA and UA where the bare GC electrode could not distinguish between the four species and all four species showed a single peak at the same potential for a mixture of 50 μM DA, 500 μM 5-HT, 1 mM AA and 0·1 mM UA (figure not shown).[33,34]

Figure 10b shows the DPVs recorded for a mixture of DA and 5-HT at the GC/Nf/Pt_{nano} electrode in the presence of AA and UA. The voltametric response observed for the mixture at the GC/Nf/Pt_{nano} electrode is dramatically increased and a large increase in the anodic peak current is observed when compared to GC/Nf electrode (figure 10a).[33,34]

Figure 11 shows the schematic representation of selective electrocatalytic oxidation of cationic DA at the GC/Nf/Pt_{nano} electrode in the presence of anionic molecules such as A and UA. Figure 11 also explains the electron-mediating properties of Pt_{nano} towards the oxidation of DA in the presence of interferences such as AA and UA.

The application of GC/Nf/Pt_{nano} electrode for the detection and determination of DA in practical samples such as dopamine injection solution (DHI) and blood plasma was tested.[34] Under the optimum conditions, the DPV peak currents were linearly related to DA concentration over the range from $1{\cdot}0 \times 10^{-8}$ to $1{\cdot}4 \times 10^{-6}$ M. A detection limit of 8 nM was estimated at a signal-to-noise ratio of **3**. DA was repeatedly determined in DHI samples with duplicate samples and the relative standard deviation was found to be 4·5%. Interference studies were carried out with species such as AA and UA. Figure 12 shows the DPVs recorded using the GC/Nf/Pt_{nano} electrode for blood plasma samples and spike addition of 10 μM DA in blood plasma in 0·1 M phosphate buffer. The recovery of DA and its metabolites in blood plasma (figure 12a) were calculated by spike addition with varying amounts of DA (figure 12b). Reproducibility of results was checked with three determinations.

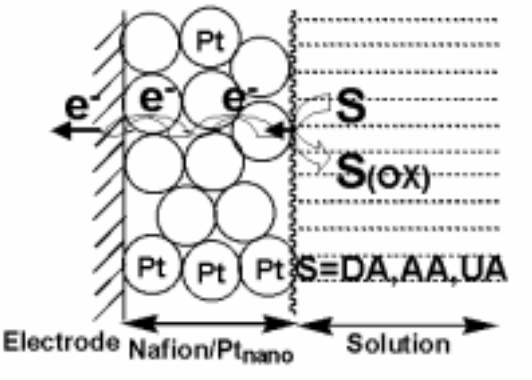

Figure 11. Schematic representation of oxidation of DA at the GC/Nf/Pt_{nano} electrode in the presence of interfering molecules such as AA and UA.

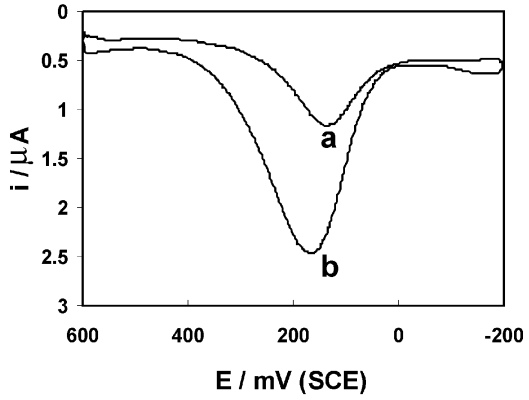

Figure 12. DPVs recorded at GC/Nf/Pt_{nano} for blood plasma sample (a), spike addition of 10 μM DA (b) in 0·1 M phosphate buffer.

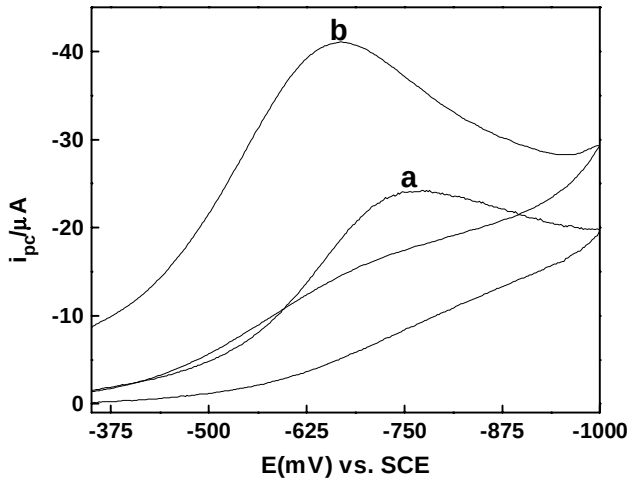

Figure 13. Cyclic voltammograms recorded at plain GC (a) and GC/Nf/Cu_{nano} (b) electrodes in O_2 saturated 0·1 M PBS. Cu_{nano} was deposited at an applied potential of –0·4 V (SCE).

6. Oxygen reduction at nanostructured Cu modified electrode

Figure 13 shows the cyclic voltammograms recorded for O_2 reduction at plain GC electrode (figure 13a) and after Cu_{nano} is incorporated into Nf film-coated GC electrode (figure 13b) in O_2 saturated 0·1 M PBS.[34,35] Under deaerated condition, the GC electrode did not show any reduction peak in the potential region –1·0 to –0·35 V. When the solution was saturated with oxygen, a reduction peak was observed in the voltammogram (figure 13). The O_2 reduction peak was observed at –0·76 V at plain GC electrode in 0·1 M PBS. At GC/Nf/Cu_{nano} electrode O_2 reduction occurs at –0·63 V with an increase in the reduction peak current and a decrease in overpotential when compared to plain GC electrode. This result suggests that the GC/Nf/Cu_{nano} electrode could be used for catalytic O_2 reduction in neutral solution. It is reasonable to conclude that the major contribution to the peak current comes from the catalytic O_2 reduction at GC/Nf/Cu_{nano} electrode. Cu_{nano} deposited at –0·4 V on the modified electrode leads to the formation of multilayer copper nanostructures on the electrode surface. The Cu_{nano} modified electrode prepared at –0·4 V showed better electrocatalytic behavior towards O_2 reduction.[34,35]

In our laboratory, further work is in progress to design metal nanoparticles modified electrodes coupled with permselective membranes for the simultaneous detection and determination of biomolecules and for the electrocatalytic reduction of O_2 and H_2O_2.

Acknowledgements

Financial support from the Department of Science and Technology (DST) and Council of Scientific and Industrial Research (CSIR), New Delhi is gratefully acknowledged.

References

1. Fendler J H (ed.) 1998 *Nanoparticles and nanostructured films* (Weinheim: Wiley-VCH)
2. Wieckowski A, Savinova E R and Vayenas C G (eds) 2003 *Catalysis and electrocatalysis at nanoparticle surfaces* (New York: Marcel Dekker)
3. Trasatti S 1994 in *Electrochemistry of novel materials* (eds) J Lipkowski and P N Ross (New York: VCH) Ch. 5
4. Zhou B, Hermans S and Somerjai G A (eds) 2004 In *Nanotechnology in catalysis* (London: Kluwer Academic/Plenum) vol. 1 & 2
5. Welch C M and Compton R G 2006 *Anal. Bioanal. Chem.* **384** 601
6. Hrapovic S, Liu Y, Male E B and Luong J H T 2004 *Anal. Chem.* **76** 1083
7. Karyakin A A, Puganova E A, Budashov I A, Kurochkin I N, Karyakina E E, Levchenko V A, Matveyenko V N and Varfolomeyev S D 2000 *Anal. Chem.* **76** 474
8. D'Souza L and Sampath S 2000 *Langmuir* **16** 8510
9. Mauritz K A and Moore R B 2004 *Chem. Rev.* **104** 4535
10. Sirk A H C, Hill J M, Kung S K Y and Birss V I 2004 *J. Phys. Chem.* **B108** 689
11. Tan S, Laforgue A and Belanger D 2003 *Langmuir* **19** 744
12. Jia N, Lefcbvre M C, Halfyard J, Qi Z and Pickup P G 2000 *Electrochem. Solid State Lett.* **3** 529
13. Martin C R 1994 *Science* **266** 1961
14. Yin Y, Shen Y and Dong S 2004 *J. Phys. Chem.* **B108** 8142
15. Tong Y, Rice C, Wieckowski A and Oldfield E 2000 *J. Am. Chem. Soc.* **122** 1123
16. Collman J P, Denisevich P, Konai Y, Marrocco M, Koval C and Anson F C 1980 *J. Am. Chem. Soc.* **102** 6027
17. Sawyer D T 1991 *Oxygen chemistry* (New York: Oxford University Press)
18. Kinoshita K 1992 *Electrochemical oxygen technology* (New York: Wiley)
19. Srinivasan S and Bockris J O M 1969 *Fuel cells: their electrochemistry* (New York: McGraw-Hill)
20. Shukla A K and Raman R K 2003 *Annu. Rev. Mater. Res.* **33** 155
21. Rubinstein I and Bard A J 1980 *J. Am. Chem. Soc.* **102** 6641
22. Bose C S C and Rajeshwar K 1992 *J. Electroanal. Chem.* **333** 235
23. Kost K M, Bartak D E, Kazee B and Kuwana T 1990 *Anal. Chem.* **62** 151
24. Gonon F, Buda M, Cespuglio R, Jouret M and Pujol J-F 1980 *Nature* (*London*) **286** 902
25. Wightman R M, May L J and Michael A C 1988 *Anal. Chem.* **60** 760A
26. Adams R N 1976 *Anal. Chem.* **48** 1128A
27. Sternson A W, Mccreery R, Feinberg B and Adams R N 1973 *J. Electroanal. Chem.* **46** 313
28. Gerhardt G A, Oke A F, Rice M E and Adams R N 1984 *Brain Res.* **290** 390
29. Zen J-M and Chen P-J 1997 *Anal. Chem.* **69** 5087
30. Rubianes M D and Rivas G A 2001 *Anal. Chim. Acta* **440** 99
31. Premkumar J and Ramaraj R 1997 *J. Solid State Electrochem.* **1** 172
32. Premkumar J 1997 Ph D thesis, Madurai Kamaraj University, Madurai
33. Selvaraju T and Ramaraj R 2005 *J. Electroanal. Chem.* **585** 290

34. Selvaraju T 2005 Ph D thesis, Madurai Kamaraj University, Madurai
35. Selvaraju T and Ramaraj R 2005 *Pramana-J. Phys.* **65** 713
36. Jiang J and Kucernak A 2004 *J. Electroanal. Chem.* **567** 123
37. Martin C R, Rubinstein I and Bard A J 1982 *J. Am. Chem. Soc*. **104** 4817
38. Grim R E 1969 *Clay mineralogy* (New York: McGraw-Hill)
39. Dong S and Qiu Q 1991 *J. Electroanal. Chem.* **314** 223
40. Wagner D 1990 in *Practical surface analysis* 2nd edn (eds) D Briggs and M P Scah (Chichester: Wiley) vol 1, appendix 5
41. Bard A J and Faulkner L R 2001 *Electrochemical methods, fundamentals and applications* (New York: Wiley)
42. Sarkar D K, Zhou X J, Tannous A and Leung K T 2003 *J. Phys. Chem.* **B107** 2879
43. Yeager E 1984 *Electrochim. Acta* **29** 1527